Journal of Controlled Release 283 (2018) 223–234

Contents lists available at ScienceDirect

Journal of Controlled Release

journal homepage: www.elsevier.com/locate/jconrel

Antitumor effect of oncolytic virus and paclitaxel encapsulated in extracellular vesicles for lung cancer treatment

M. Garofalo[a,b,*], H. Saari[a,1], P. Somersalo[a,b,1], D. Crescenti[b], L. Kuryk[a,c,d], L. Aksela[a], C. Capasso[e], M. Madetoja[f], K. Koskinen[g], T. Oksanen[a], A. Mäkitie[h], M. Jalasvuori[a,g], V. Cerullo[e], P. Ciana[b], M. Yliperttula[a,*]

[a] Division of Pharmaceutical Biosciences and Centre for Drug Research, University of Helsinki, Viikinkaari 5, Helsinki 00790, Finland
[b] Department of Oncology and Hemato-Oncology, Center of Excellence on Neurodegenerative Diseases, University of Milan, Via Balzaretti 9, Milan 20133, Italy
[c] National Institute of Public Health – National Institute of Hygiene, Department of Virology, 24 Chocimska str, 00-791 Warsaw, Poland
[d] Targovax Oy, R&D, Clinical Science, R&D, Saukonpaadenranta 2, 00180 Helsinki, Finland
[e] Laboratory of ImmunoViroTherapy, Drug Research Program, Faculty of Pharmacy, University of Helsinki, Viikinkaari 5, Helsinki 00790, Finland
[f] Made Consulting, Tykistökatu 4 B, FI-20520 Turku, Finland
[g] Biological and Environmental Science, Nanoscience Center, University of Jyväskylä, Survontie 9C, 40500, Finland
[h] Department of Otorhinolaryngology – Head and Neck Surgery, Helsinki University Hospital and University of Helsinki, P.O.Box 263, FI_00029 HUS, Helsinki, Finland

ARTICLE INFO

Keywords:
Extracellular vesicles
Oncolytic viruses
Cancer therapy
Drug delivery
Paclitaxel
Xenograft animal model
Lung cancer

ABSTRACT

Standard of care for cancer is commonly a combination of surgery with radiotherapy or chemoradiotherapy. However, in some advanced cancer patients this approach might still remaininefficient and may cause many side effects, including severe complications and even death. Oncolytic viruses exhibit different anti-cancer mechanisms compared with conventional therapies, allowing the possibility for improved effect in cancer therapy. Chemotherapeutics combined with oncolytic viruses exhibit stronger cytotoxic responses and oncolysis. Here, we have investigated the systemic delivery of the oncolytic adenovirus and paclitaxel encapsulated in extracellular vesicles (EV) formulation that, *in vitro*, significantly increased the transduction ratio and the infectious titer when compared with the virus and paclitaxel alone. We demonstrated that the obtained EV formulation reduced the *in vivo* tumor growth in animal xenograft model of human lung cancer. Indeed, we found that combined treatment of oncolytic adenovirus and paclitaxel encapsulated in EV has enhanced anticancer effects both *in vitro* and *in vivo* in lung cancer models. Transcriptomic comparison carried out on the explanted xenografts from the different treatment groups revealed that only 5.3% of the differentially expressed genes were overlapping indicating that a *de novo* genetic program is triggered by the presence of the encapsulated paclitaxel: this novel genetic program might be responsible of the observed enhanced antitumor effect. Our work provides a promising approach combining anticancer drugs and viral therapies by intravenous EV delivery as a strategy for the lung cancer treatment.

1. Introduction

Despite major advances in conventional cancer treatments with surgery, radiotherapy, chemotherapy,and their combination, the outcome is still partially ineffective against numerous cancer types, like lung cancer [1]. Lung cancer is highly invasive and rapidly metastasizing, often diagnosed at an advanced stage with poor prognosis and without efficient treatment options [2]. Given the poor survival rate of patients, new therapeutic strategies with systemic drug delivery are warranted. Oncolytic virotherapy is emerging as a promising and potential approach to treat cancer, and the approval of the first oncolytic virus, Imlygic (T-Vec, talimogene laherparepvec), in the Western world by US Food and Drug Administration (FDA) and European Medicines Agency (EMA) provides new perspectives for improved treatment of cancer [3, 4]. Indeed, its application can be particularly relevant for tumors without curative options, including metastatic lung cancers [1]. In oncolytic virus therapy, viruses are specifically engineered to preferentially infect, replicate in and kill cancer cells instead of normal cells where their normal functions are restricted [5–9]. Virus replication in tumor cells eventually leads to cell lysis, allowing

* Corresponding authors at: Division of Pharmaceutical Biosciences and Centre for Drug Research, University of Helsinki, Viikinkaari 5, Helsinki 00790, Finland.
E-mail addresses: mariangela.garofalo@helsinki.fi (M. Garofalo), marjo.yliperttula@helsinki.fi (M. Yliperttula).
[1] Shared co-authorship.

https://doi.org/10.1016/j.jconrel.2018.05.015
Received 21 December 2017; Received in revised form 10 May 2018; Accepted 14 May 2018
Available online 01 June 2018

the new virus progeny to spread to surrounding cells and even to distant metastases through circulation [10]. However, as a single therapeutic agent oncolytic adenoviruses have not been observed to efficiently destroy large tumor mass in patients [11, 12]. Thus there is a need to enhance their antitumor efficacy by combining viral therapy with other anticancer agents [13–15]. Cisplatin has improved oncolysis of Herpes simplex virus type 1 (HSV-1) in non small cell lung cancer (NSCLC) [16]. Additionally, combination of cisplatin with adenovirus facilitated the replication of the virus and significantly reduced the tumor progression [17]. Enhanced effects have been also reported in a malignant pleural mesothelioma (MPM) with NV1066 (HSV-1 based virus) [18]. However, the use of oncolytic viruses as a potential approach to treat cancer has also disadvantages [19]; the immune response will presumably limit ongoing viral replication and spread in cancer cells. Administered viruses will be detected by immune system and inactivated by neutralizing antibodies, decreasing its replication and efficacy. Additionally, given the intratumoral administration of oncolytic viruses [20–22], they are eligible only in injectable lesions and thus limiting the approach to treat many solid tumors. Systemic delivery of virus together with anticancer drugs would circumvent some of these limitations. Extracellular vesicles (EVs) are naturally occurring cargo delivery agents with the potential to be used as drug delivery vehicles [23, 24] since they can transfer biological molecules even over long distances within the body [25]. The lipid membrane of EVs can protect the cargo from degradation by body fluids and further improved uptake by the target cells [26, 27]. In recent studies, it has been shown to that oncolytic viruses can be delivered into the nucleus of tumorigenic cells by tumor microparticles while simultaneously avoiding the production of neutralizing antibodies and mediating the virus entry into cancer cells independently from the virus-specific receptor [28].

In this study, we set to investigate whether it is possible to encapsulate the oncolytic adenovirus and chemotherapeutic agent into EVs in an attempt to utilize them as carriers for targeted drug delivery. The obtained formulations were tested *in vitro* in lung cancer cell line and subsequently *in vivo* in lung cancer xenograft animal model using both intra tumor (it) and intra venous (iv) injections. Abraxane (paclitaxel, albumin-bound nanoparticle formulation) and EVs without encapsulated virus and/or drug were used as control samples. We found that the systemic delivery of both oncolytic virus and paclitaxel encapsulated in EVs resulted in improved drug efficacy and reduced off-target toxicity.

2. Materials and methods

2.1. Cell culture

A549 human lung cancer cell line was purchased from the American Type Culture Collection (ATCC, USA). The cells were cultured at 37 °C and 5% CO_2 in Dulbecco's modified eagle medium (DMEM, Lonza, Switzerland) supplemented with 10% fetal bovine serum (FBS, Gibco Laboratories, USA), 1% of 100 u/mL penicillin/streptomycin (Gibco Laboratories) and 1% L-glutamine (Gibco Laboratories).PNT2 (European Collection of Authenticated Cell Cultures, ECACC, UK) human prostate cell line was purchased from Sigma-Aldrich. The cells were cultured at 37 °C and 5% CO_2 in RPMI 1640 (Gibco Laboratories) supplemented with 10% FBS (Gibco Laboratories), 1% of 100 u/mL penicillin/streptomycin (Gibco Laboratories) and 2% L-glutamine (Gibco Laboratories). The prostate cancer cell line PC-3 (ATCC), was cultured at 37 °C and 5% CO_2 in Ham's F-12 K (Kaighn's) basal medium (Gibco Laboratories) supplemented with 10% FBS (Gibco Laboratories) and 1% of 100 u/mL penicillin/streptomycin (Gibco Laboratories).

2.2. Oncolytic virus

Ad5D24-CpG, was generated according to standard protocols [29] by recombining a CpG-rich shuttle plasmid (pTHSN-CpG1) with a plasmid containing the 24 adenovirus backbone. Viral stocks were expanded in human lung cancer cell line A549 and purified on cesium chloride gradients. The viral particle concentration was determined by OD_{260}-reading and standard $TCID_{50}$ (tissue culture infectious dose 50) assay was performed to determine infectious particle titer. Virus was characterized by PCR and restriction enzyme analysis Ad5D24-RFP, expressing a red fluorescent protein (RFP) was kindly provided by Dr. Masataka Suzuki from Baylor College of Medicine (Houston, TX [30];).

2.3. Paclitaxel (PTX) solutions

A 50 mM stock solution of Paclitaxel (PTX; Selleck Chemicals) was prepared by dissolving PTX into di-methyl sulfoxide (DMSO) (Sigma-Aldrich). This was used as the stock solution in A549 cell experiments as well as in EV-encapsulation of PTX.Abraxane was provided for us by the Hospital Pharmacy of the Helsinki University Hospital based on the prescription of MD A. Mäkitie, School of Medicine, University of Helsinki, Finland. A stock suspension of Abraxane (Albumin-PTX conjugate, Celgene, USA) was prepared by suspending the powder, corresponding to 100 mg of PTX, in phosphate buffer saline (PBS, Lonza) to a final volume of 8.5 mL, resulting in 11.76 mg/mL of PTX. This stock was then further diluted in PBS to produce the solutions used in the *in vivo* animal experiments exclusively.

2.4. Production of extracellular vesicles (EV) and PTX loaded EVs formulations

In order to produce EVs 2.6×10^6 A549 cells were plated into T-175 flask in medium supplemented with 5% FBS. The FBS growth media was ultra-centrifuged overnight (110,000 $\times g$ at 4 °C for 18 h, Optima LE-80 K ultracentrifuge, rotor type 50.2, Beckman Coulter) to remove EVs present in serum. Cells were cultured at 37 °C and 5% CO_2 until cytopathic effect was seen, where upon the media was collected.

EVs were isolated from the conditioned medium using differential centrifugation. First the conditioned medium was centrifuged at 500 $\times g$ in 4 °C for 10 min to pellet cells (Allegra X-15R Centrifuge, Beckman Coulter). Then, the supernatant was collected and ultra-centrifuged for 2 h at 100000 $\times g$ in 4 °C, using Optima L-80 XP ultra-centrifuge (Beckman Coulter) with rotor SW32Ti (Beckman Coulter). The supernatant was aspirated and EV- containing pellets containing re-suspended in PBS (Lonza) 100 μL and stored at −80 °C.

PTX-loaded EVs were prepared as previously described by us [23] by incubating 1×10^8–5×10^9EVs in 1 mL of 5 μM PTX-DPBS solution for *in vitro* samples and 10 μM PTX-DPBS solution for *in vivo* samples, for 1 h at 22 °C. Next, the samples were centrifuged at 170000 $\times g$ for 2 h to pellet the EVs. The supernatant containing unbound PTX was removed, and the EV-pellet was washed by suspending it in DPBS and pelleting it again at 170000 $\times g$.

2.5. Production of EV-Virus and EV-Virus-PTX formulations

In order to produce EV-encapsulated virus (EV-Virus), 2.6×10^6 of A549 cells were infected with with 10 viral particles/cell of Ad5D24CpG and were cultured at 37 °C and 5% $CO_2$48 h later when most of the cells were detached from the culture flask, the culture media were collected for EV-Virus isolation using differential centrifugation. First the conditioned medium was centrifuged at 500 $\times g$ and 4 °C for 10 min, to separate the cells (Allegra X-15R Centrifuge, Beckman Coulter). Then, the supernatant containing EV-Virus was collected and ultra-centrifuged for 2 h at 100000 $\times g$ and 4 °C, using Optima L-80 XP ultra-centrifuge (Beckman Coulter) with rotor SW32Ti (Beckman Coulter). The supernatant was aspirated and pellets containing EV-Virus re-suspended in PBS 100 μL and stored at −80 °C.EV-Virus samples were incubated in 100 mM NaOH at room temperature for 20 min in order to inactivate any free not EV encapsulated virus present. Free virus used as controls was always inactivated for each

experiment performed as previously reported [31]. Samples were subsequently neutralized by the addition of HCl 0.1 M.

To generate EV-Virus-PTX, the EV-Virus formulation was incubated in a 10 μM PTX solution, prepared by diluting 10 mM PTX in DMSO with PBS with the ratio of 1:1000. Incubation was carried out at RT with mixing for 1 h. Samples were then centrifuged at 150000 ×*g* for 2 h at RT, in order to pellet EV-Virus-PTX. The washing procedure was repeated using PBS as diluent. The final EV-Virus-PTX pellet was re-suspended in 100 μL of PBS and stored at −80 °C.

2.6. Quantification of PTX present in EV-Virus-PTX

50 μL of 1.5×10^{10} EV-Virus-PTX/mL as well as supernatant from the second washing step associated with removal of free PTX, to enable validation of the washing procedure, was processed for ultra performance liquid chromatography (UPLC, Acquity UPLC System) using a Cortecs UPLC C18+ column, 2.1 × 50 mm, particle size 2.7 μm (Waters, USA). Additionally, a 10 μM PTX solution was prepared, and used as a control for sample processing. Sodium dodecyl sulfate (SDS) was added to samples to a final concentration of 5% (*w/v*) in order to lyse EV-Virus PTX. Vortexing was followed by incubation at RT for 1 h. Acetonitrile was then added to a final concentration of 75% (*v*/v) and samples vortexed. Precipitated proteins were pelleted by centrifugation at 10000 ×*g* for 5 min at RT. The supernatant was analyzed by UPLC using gradient flow of acetonitrile from 30% to 80% in phosphate buffer, pH = 2, at 30 °C within 3 min. Detection and quantification of PTX, with a retention time of 1.7 min, was performed spectrophotometrically at the wavelength of 229 nm by using a reference standard curve.

2.7. Size distribution analysis by nanoparticle tracking analysis (NTA)

Size distribution and concentration of EV, EV-Virus and EV-Virus-PTX formulations were analyzed by NTA using Nanosight model LM14 (Nanosight) equipped with blue (404 nm, 70 mV) laser and sCMOS camera. The samples containing virus were incubated at +95 °C for 10 min in order to inactivate the viruses. NTA was performed for each sample by recording three 90 s videos, subsequently analyzed using NTA software 3.0 (Nanosight). The detection threshold was set to level 5 and camera level to 15.

2.8. Zeta potential analysis by electrophoretic light scattering

The zeta potential was measured using ZetaSizer Nano (Malvern, UK). All the samples were diluted in a volume of 800 L of MilliQ H_2O and injected with a 1 mL syringe in the capillary flow (DTS1070 folded capillary cell) for the measurement. An equilibration time of 120 s was set on the software to allow the samples to stabilize at 25 °C inside the measurement chamber. Three parallel measurements were performed on each sample.

2.9. HIM microscopy

For Helium Ion Microscopy, A549 cells were cultured to 70% confluence in DMEM (Gibco Laboratories, USA) supplemented with heat inactivated 10% FBS (Gibco Laboratories) and 100 u/mL penicillin-streptomycin (Gibco Laboratories) on poly-L-lysin (Sigma Aldrich, Germany) glass coverslips. Cells in culture were infected with EV-Virus (5×10^9/mL on 75 cm^2 80% confluent cell culture) by replacing the cell culture medium with a solution containing EV-Virus in DMEM of 2% FBS and 100 u/mL penicillin-streptomycin. After 2 h incubation, EV-Virus solution was again replaced with DMEM of 10% FBS and 100 μ/mL penicillin-streptomycin. Cells were fixed at different time points by replacing the EV-Virus solution with 2% glutaraldehyde (GA, Merck, USA) in 0.1 M Sodium Cacodylate (NaCac) buffer (pH 7.4). After GA fixation, the cells were washed twice with 0.1 M NaCac and further fixed with 1% OsO_4 in 0.1 M NaCac buffer (pH 7.4). After 1 h in OsO_4, cells were washed twice with 0.1 M NaCac buffer and chemically dried in an increasing EtOH concentration series of 50%, 70%, 96%, and twice with 100%. After 100% EtOH, the cells were submerged in 98% hexamethyldisiloxane (Sigma Aldrich) and left to dry for overnight. After fixation and chemical drying, coverslips were mounted on stands and imaged with Orion NanoFab Helium Ion Microscope (Zeiss, Germany) using 30 kV acceleration voltage with beam current 0.2–1 pA.

2.10. Transduction assay

Cells were seeded at a density of 1×10^4 cells/well in 96-well plates and maintained under appropriate condition. On the following day cells were treated in triplicates with an oncolytic adenovirus Ad5D24Rfp encoding for the red fluorescent protein (10vp/cell) and control EVs (10 particles/cell), EV-Virus (10 particles/cell), EV-PTX (10 particles/cell, 5 μM of PTX), EV-Virus-PTX (10 particles/cell, 5 μM of PTX) or Virus and PTX separately (Virus + PTX) (10 vp/cell, 5 μM of PTX). EVs, EV-Virus and EV-Virus-PTX had the same doses of particles as virus alone (10 vp were calculated as 10 EV-particles per cell in the well). The cells were then imaged with EVOS FL fluorescence microscope at 8, 24 and 48 h after the treatment in order to count the portion of cells expressing RFP.

2.11. Immunocytochemistry staining (ICC)

The determination of the infectivity was based on the visual quantification of infected cells as previously described [32, 33]. Cells were seeded at a density of 2×10^5cells/well in 24 well plates, and maintained under appropriate condition in DMEM, completed with 5% FBS, 1% L-glutammine and 1% of penicillin/streptomycin. All the chemicals were purchased from Gibco Laboratories. On the following day cells were treated with Virus (10vp/cell), Virus + PTX (10vp/cell and 5 μM PTX solution), EV-Virus formulations (10 particles/cell) and EV-Virus-PTX formulations (10 particles/cell, 5 μM of PTX).

Plates were centrifuged for 90 min with 1000 ×*g* in 37 °C and incubated for 48 h before staining at 37 °C and 5% CO_2.48 h following the incubation cells were fixed by adding 250 μL of ice-cold methanol per well and incubated 15 min. Then cells were washed three times with PBS 1%-BSA (Bovine serum albumin, 9048-46-8 Sigma-Aldrich) solution and incubated in the dark for one hour with 1st antibody, mouse monoclonal anti-hexon 1:2000 (Novus Biological, NB600-413). After the incubation time, cells were washed three times with PBS 1%-BSA and incubated in the dark for other 1 h with 2nd antibody: Biotin-SP-conjugated goat anti-mouse 1:500 (Jackson Immuno Research, 115-065-062). After the incubation time, cells were washed three times with PBS1%-BSA and incubated in the dark for 30 min with extravidin-peroxidase (Sigma Aldrich, E2886). Finally cells were washed three times as indicated earlier and treated with Dab peroxidase substrate solution (Sigma Aldrich, A7284-50ML). To quench the reaction, cells were treated once with PBS. The detection of the infectious titer was performed using microscope EVOS, and each well was photographed with 5 pcs at 5 non-overlapping sites. The following formula was used to determine the infectious titer:

$$\text{Infectious titer:} x\frac{A(\text{well})}{A(\text{field})}\frac{1}{L}\frac{1mL}{v}$$

Where x = number of infected (stained cells).
A(24 well) = 190 mm^2.
A(field) = surface area of the field.
L = dilution.
v = volume of virus dilution applied per well.

2.12. MTS cell viability assay

A549, PNT2 and PC-3 cells were seeded at a density of 1×10^4cells/well in 96-well plates and maintained under appropriate condition. On the following day cells were treated in triplicates with Virus (10vp/cell), Virus + PTX (10vp/cell + 5 μM PTX solution), control EVs (10 particles/cell), EV-PTX (10 particles/cell, 5 μM of PTX), EV-Virus formulations (10 particles/cell), EV-Virus-PTX formulations (10 particles/cell, 5 μM of PTX). Cell viability was determined by MTS assay according to the manufacturer's protocol (Cell Titer 96 AQueous One Solution Cell Proliferation Assay; Promega, Nacka, Sweden). The absorbance was measured with a 96-wells plate spectrophotometer Varioskan Flash Multimode Reader (Thermo Scientific) at 490 nm. The experiments were independently performed three times with triplicates of each condition in each experiment.

2.13. Analysis of apoptotic and necrotic cells

A549 cells were plated into 6 well plates, 2×10^5cells/well. Cells were treated with an oncolytic adenovirus Ad5D24CpG 10 vp/cell, Virus + PTX (10vp/cell + 5 μM PTX solution), control EVs (10 particles/cell), EV-PTX (10 particles/cell, 5 μM of PTX), EV-Virus formulations (10 particles/cell), EV-Virus-PTX formulations (10 particles/cell, 5 μM of PTX). The amount of apoptotic and necrotic cells was measured after 24 h post-treatment with a TACS Annexin V-FITC kit (Trevigen Inc., Gaitherburg, MD, US) and BD LSRII flow cytometer according to the manufacturer's instruction.

2.14. In vivo xenograft animal experiments

FIRST DAY OF TREATMENT Day 0	SECOND DAY OF TREATMENT Day 2	THIRD DAY OF TREATMENT Day 4	FOURTH DAY OF TREATMENT Day 15
EVs ($1x10^9$particles/tumor)	**X**	**X**	**X**
Virus ($1x10^8$ vp/tumor)	**X**	**X**	**PBS**
Abraxane (10 mg of PTX/kg)	**PBS**	**PBS**	**X**
Virus+Abraxane ($1x10^8$ vp/tumor +10 mg of PTX/kg)	**X**	**X**	**X**
EV-Virus ($1x10^8$ particles/tumor + $1x10^8$ vp/tumor)	**X**	**X**	**PBS**
EV-Virus-PTX ($1x10^8$ particles/tumor including $1x10^8$ vp/tumor, and 10 mg of PTX/kg)	**X**	**X**	**X**

All the animal experiments performed under the ethical permission (ESAVI/10482/04.10.07/2015) of the National Laboratory Animal Board of Finland (Care and Use Committee) by Made Consulting Ltd. Oy (Turku, Finland) in GLP level animal facility.

Mice were obtained from Janvier Labs (Barrier 4E-1, France) at 4 weeks of age. The acclimatization period was 13 days prior to A549 cancer cell injections, the cell line was the same used for the *in vitro* cell experiments. The A549 cell line purity was tested usingby IDEXX BioResearch - IMPACT III panelbefore inoculation and the cells viability of 99% were detected 50 min prior to first inoculation and 90% 20 min after the last inoculation using NucleoCounter NC-200. Health status of the mice was monitored daily and as soon as signs of pain or distress were evident they were euthanized. For the efficacy experiment, human xenografts were established by injecting 1.5×10^6 A549 cells s.c. into the flanks of 6-week old female BALB/c nude mice. The treatment groups were as follows: Virus (n = 6); Virus + Abraxane (n = 6); Abraxane (n = 6); EV (n = 6) and EV-Virus (n = 9); EV-Virus-PTX (n = 9). Treatment groups were administered i.v (100 μL) and i.t (50 μL) to mice with tumors (one tumor per mouse about 5 mm in diameter). The dosing days were 0, 2, and 4 for Virus (according to previous protocols [29]) and EV-Virus; 0 and 15 for Abraxane as previously reported [34]; 0, 2, 4 and 15 for EV and EV-Virus-PTX (table above and the Supplementary Table 1). The equation: $0.52 \times \text{length} \times (\text{width})^2$, was used to calculate the tumor volumes to study the efficacy of the used EV-formulations. However, the average diameter of 15 mm was used as a limit to euthanize mice.Tumors, livers and spleens from each mouse were collected for histopathological examinations.

2.15. Quantitative PCR

qPCR for adenovirus E4 copy number was carried out according to the protocol previously described [35] (primer FW:50-GGA GTG CGC CGA GAC AAC-30, primer RV: 50-ACT ACG TCC GGC GTT CCA T-30, probe E4: 50-(6FAM)-TGG CAT GAC ACT ACG ACC AAC ACG ATC T-(TAMRA)230). Total DNA was extracted from BALB/c nude murine samples (tumors, livers, blood) using the QIAamp DNA Blood Mini Kit (Qiagen, Hilden, Germany) according to manufacturer's protocol. Subsequently isolated DNA was analyzed for adenoviral E4 copy number normalized to murine beta-actin (liver, blood) and human beta-actin (tumor), respectively ((primer FW: 50-CGA GCG GTT CCG ATG C-30, primer RV: 50-TGG ATG CCA CAG GAT TCC AT-30, probe murine beta-actin: 50-(6FAM)-AGG CTC TTT TCC AGC CTT CCT TCT TGG-(TAMRA) 230; (primer FW: 50-CAG CAG ATG TGG ATC AGC AAG-30, primer RV: 50- CTA GAA GCA TTT GCG GTG GAC-30, probe human beta-actin: 50-(6FAM)- AGG AGT ATG ACG CCG GCC CCT C-(TAMRA)230). Samples were analyzed using LighCycler qPCR machine (LighCycler 480, Roche, Basel, Switzerland).

2.16. Histopathological studies

Left lateral lobe of liver, half of spleen and one lobe of lungs were

taken into 4% buffered formalin at necropsy. Finnish Centre for Laboratory Animal Pathology, Helsinki, Finland performed the histopathological evaluations of the lung, liver, spleen and tumor *in vivo* samples of nude (athymic) mice, implanted with human tumor xenograft and treated with virus alone, control EVs and EV-Virus-PTX by histotechnology. The samples were embedded into paraffin, cut at 4 μm (spleen 3 μm), and stained with haematoxylin and eosin. The histopathological evaluation was performed as a blind using 40× magnification using the microscope Zeiss Axio Imager.A2, Carl Zeiss Microscopy GmbH, Jena, Germany.

2.17. Total RNA-sequencing

RNA from tumor tissues, from mice treated with control EVs, EV-Virus and EV-Virus-PTX, were extracted using RNeasy Plus Micro Kit (Qiagen) according to the manufacturer's instructions. Indexed libraries were prepared from 10 ng/ea. purified RNA with SMARTer Stranded Total RNA-Seq Kit - Pico Input Mammalian (Clontech Laboratories, Inc.) according to the manufacturer's instructions. Libraries were quantified using the TapeStation 4200 (Agilent Technologies) and pooled such that each index-tagged sample was present in equimolar amounts, with final concentration of the pooled samples of 2 nM. The pooled samples were subject to cluster generation and sequencing using an Illumina NextSeq 500 System (Illumina) in a 2 × 150 single read format at a final concentration of 1.8 pmol.

2.18. RNA-Seq Analysis

The raw sequence files generated (fastq files) underwent quality control analysis using FastQC (http://www.bioinformatics.babraham.ac.uk/projects/fastqc/).To analyze RNA-Seq data we used the strategy called “Direct mapping” as previously described [36]. Reads were first mapped on human genome (assembly hg38) using STAR [37]. The quantification of transcripts expressed for each replicate of the sequenced samples was performed using HTSeq-count [38]. R was used to create a matrix of all transcripts expressed in all samples with the corresponding read-counts and the Bioconductor package *limma* [39] was used to normalize the data and then to perform the differential expression analysis: an Empirical Bayes moderation *t*-test was performed.Data were also normalized in FPKM (Fragments Per Kilobase Of Exon Per Million Fragments Mapped) using Cuffnorm [40]. Genes up-regulated ($\log2FC \geq 1$) and down-regulated ($\log2FC \leq -1$) with a *P*-value < 0.05 were selected as differentially expressed. From these lists of DEGs, Genesis software [41, 42] was used to generate heat maps and to investigate the gene ontology (GO) terms in the two gene sets of differentially expressed genes.

2.19. Statistical analysis

Statistical analysis was performed by using one-way ANOVA followed by Bonferroni post-hoc test. Survival curves and their statistical analysis were performed using Kaplan–Meier test. The *in vitro* therapeutic synergy was calculated using fractional tumor cell viability (FTV) method [43, 44]. Adjusted *P*-values in Supplementary Table 3 were calculated performing Fisher's exact test and the correction for multiple hypothesis testing using the Benjamini-Hochberg method [45]. All statistical analysis, calculations and tests were performed using GraphPad Prism 5 (GraphPad Software, San Diego, CA).

3. Results

3.1. Oncolytic adenoviruses can be encapsulated inside EVs with PTX

For investigating the possibility to create a new type of systemic drug delivery strategy for lung cancer, we encapsulated chemotherapy drug and oncolytic virus into EVs. The size distributions of EV-Virus and EV-Virus-PTX formulations were determined by using NTA (Fig 1AB). Size distribution of both control EVs and EV-Virus formulations were detected to be in the range of 50–1000 nm. The size distribution of EV-Virus overlaps with the size of the Virus (93.8 ± 4.3 nm) with most of the EVs being smalleror the same size as the virus (Fig. 1A). In addition even though heating was used to inactivate any free viruses in samples, the inactivated free virus particles are still present and this may affect the size distribution of EV-Virus, bringing it closer to the size distribution of free virus (Fig. 1A). The effect of heating on the size distribution of EVs was also assessed with A549 control EVs: while the particle count of heated EVs was within the standard error of non-boiled EVs, the size distribution shifted to slightly smaller (approximately 20 nm) after boiling, which can affect the result of EV-Virus as well (unpublished data not shown). In any case, the size distributions of EV-Virus and control EVs were very similar, with EV-Virus being slightly more oriented towards its peak at 75 nm. With EV-Virus-PTX and EV-PTX (EVs loaded with PTX), no significant size differences were seen due to the addition of PTX (Fig. 1B). Furthermore, control EVs and EV-Virus both had a similar strongly negative zeta-potential of approximately −40 mV, while the free virus had a zeta-potential of −20 mV (Fig. 1C), suggesting that EV-Virus preparation consisted mostly of EVs, otherwise it zeta-potential should have shifted towards a

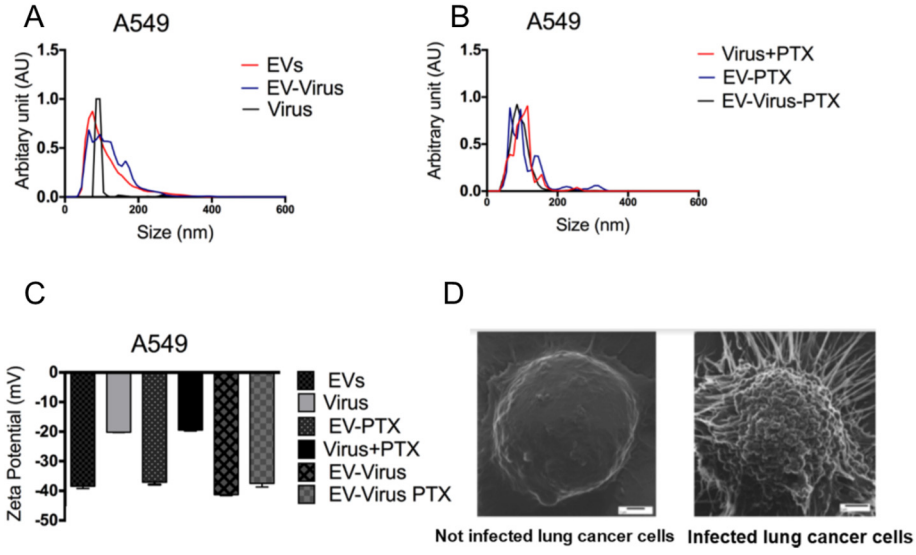

Fig. 1. Oncolytic adenovirus encapsulated into the Extracellular vesicle allows complex formation. (A-B) Size distribution of virus alone, EV-virus, EV-paclitaxel, EV-Virus-paclitaxel and Virus were determined by using Nano tracking analysis (NTA). (C) The surface charge of the virus alone, EV-virus, EV-paclitaxel, EV-Virus-paclitaxel and Virus was measured using ZetaSizer Nano Malvern. (D) Helium Ion Microscopy pictures imaged with Orion NanoFab Helium Ion Microscope (Zeiss, Germany) using 30 kV acceleration voltage with beam current 0.2–1 pA. Images are of non-infected (left) and EV-V infected (right) cells. The deformed phenotype with multiple protrusions extending from the cell surface was often observed in infected cells at least after 24 h post-infection.

less negative value. The zeta-potential was also unaltered in EV-Virus-PTX, and EV-PTX formulations, as is to be expected since PTX is a chargeless molecule (Fig. 1C).

Helium Ion Microscopy (HIM) is an imaging technique comparable to Scanning Electron Microscopy, with the distinction that samples do not require conductive coating. HIM was used to image uninfected cells as well as EV and EV-Virus infected cells in an attempt to observe potential changes due to the EV-Virus interactions on the cell surface. EV exposed cells did not appear to differ from the un-infected cells (results not shown). Yet, occasionally the surface of EV-Virus infected cells was covered with vesicle-like protrusions (Fig. 1D). This phenomenon may derive from virus-induced changes inside the cell, resulting in phenotypic alterations on the surface.

The amount of PTX encapsulated into the EVs was determined by UPLC as previously described [23] (Supplementary Table 1). The washing protocol used in the production of EV-Virus-PTX formulations were successful, since the PTX concentration of the second washing step supernatant was below 0.05 μM, and thus insignificant when compared to the PTX concentration of EV-Virus-PTX (4.7 μM). The UPLC assessed concentration of the 10 μM PTX control sample, shows a 38% loss of PTX (Supplementary Table 1). However, the concentration of the 10 mM PTX DMSO stock solution was confirmed by UPLC analysis. PTX precipitation is most likely not the reason for the PTX loss seen in the control sample, since acetonitrile was added to a final concentration of 75% to samples prior to UPLC analysis. However the analysis of PTX in EV-Virus-PTX was just meant as a qualitative proof that PTX is indeed encapsulated in the vesicles.

3.2. In vitro and in vivo enhanced antitumor effect of virus and PTX in EV-Virus and EV-Virus-PTX formulations

The responsiveness of solid tumors to chemotherapeutic agents depends to great extent of the optimization of the drug delivery. As of such, we here set to evaluate in a factorial experiment the *in vivo* efficacy of several combinations of EV-Virus-PTX formulations to alter tumor growth in a lung xenograft animal model. Abraxane is a clinically approved nanoformulation [46] chosen according to the clinical settings previously described [34] and it was introduced, since previous study showed that patients with non small cell lung cancer may benefit from the treatment [47, 48]. Nude mice bearing A549 cells originating tumor in the right flank were treated by intravenous (iv) injections on day 0, 2, 4 and 15 with: i) EVs alone (1×10^9 particles/tumor), Virus alone (1×10^8vp/tumor), Abraxane (10 mg of PTX/kg); Virus + Abraxane (1×10^8vp/tumor + 10 mg of PTX/kg); EV-Virus (1×10^8particles/tumor + 1×10^8 vp/tumor); EV-Virus-PTX formulation (1×10^8particles/tumor including 1×10^8vp/tumor, and 10 mg of PTX/kg) (Supplementary Table 2). EVs alone were not able to control the tumor growth, and were thus used as negative control in our experiments. The intratumoral (it) treatment did not show significant differences between EV-Virus, EV-Virus-PTX and Abraxane treatments (Supplementary Fig. 1).

Interestingly, the iv injection of the EV-Virus-PTX formulation significantly reduced ($P < 0.001$) tumor growth in comparison to naked virus and Virus + Abraxane (Fig. 2A). The highest survival rate was observed in EV-Virus and EV-Virus-PTX treatments (90% at 60 days) (Fig. 2B). The best survival rate (Fig. 2B) was observed in the combinatory group: EV-Virus-PTX over other studied formulations, suggesting that the best anti-tumor efficacy response was positively correlated with the survival.

The local replication of the virus was quantified by the adenovirus E4 copy number in tumor, liver and serum by qPCR analysis. Adenoviral particles were not detected in serum and liver in any of the tested groups (Fig. 2C), suggesting that EV-Virus administered intraveniously infects and replicates only in tumor cells.

In order to verify the *in vitro* cell death by the EV-Virus and EV-Virus-PTX due to the apoptotic events, the flow cytometry measurements were carried out by measuring the amount of Annexin-V (early apoptotic stage) and propidium iodide (late apoptotic stage) for positive cells at 24 h post treatment. By that we were able to confirm that EV-Virus and Virus + PTX treatments induced both early and late *in vitro* apoptotic effect in A549 cells (Fig. 2 DE) (Supplementary Fig. 2).The *in vitro* therapeutic synergy between EVs and Virus was calculated using fractional tumor cell viability (FTV) method and demonstrated synergistic antitumor effect in the EV-Virus-PTX treatment group (Fig. 2 FG).

Histopathological analysis of the liver, spleen and tumor samples from mice demonstrated no substantial changes (Fig. 3), with the exception of EV-Virus treatment, which showed moderate-sized inflammatory focus (mostly neutrophils) in otherwise normal liver lobule (Fig. 3 A4). Spleen samples displayed general histological pattern typical for nude mice such as periarteriolar lymphatic sheet areas (PALS) and in some cases mild lymphocyte hyperplasia (Fig. 3 B1–B4) [49]. Tumor samples exhibited typical features of a lung carcinoma (malignant epithelial tumor) and they were very uniform in their growth pattern and cellular features (Fig. 3 C4).

3.3. Oncolytic adenoviruses encapsulated in the EVs show increased transduction efficacy and enhanced infectious titer

The transduction assay was conducted by using the red fluorescent protein [30] expressing virus Ad5D24RFP encapsulated in EVs. The transduction efficacy of the virus Ad5D24RFP alone was compared with EV-Virus and EV-Virus-PTX.Transduction was assessed at 8, 24 and 48 h post-infection. Interestingly, already at 8 h from infection, the amount of red fluorescent cells in EV-Virus and EV-Virus-PTX treated cultures was higher compared to cells treated with Virus Ad5D24RFP after 48 h (Fig. 4AB). The infectivity of the different formulations (Virus, Virus + PTX, EV-Virus and EV-Virus-PTX) were further investigated by Immunocytochemistry Assay (ICC). The infectious titer was found to be significantly higher for EV-Virus and EV-Virus-PTX formulations when compared to cells treated with virus Ad5D24RFP alone or with Virus + PTX (Fig. 4 CD).

3.4. Oncolytic adenoviruses encapsulated in the EVs show enhanced cytotoxicity

To ensure that the cancer derived EVs did not affect healthy cells at least during the period of 48–96 h, in which we saw a clear anticancer effect in cancer cells, we performed the experiments also with the PNT2 cells, which is a non-cancerous cell line of prostate epithelium. It was shown by MTS cell viability assay (Fig. 5A).

Then cytotoxicity of the EV-formulations was studied by MTS cell viability assays on the A549 cell line. EV-Virus and EV-Virus-PTX formulations reduced cell viability significantly more when compared to cells treated with the virus alone (Fig. 5B) ($p < 0{,}001$). Indeed, the cell killing activity of EV-Virus and EV-Virus-PTX formulations was investigated by the MTS cell viability assays on A549 and PC-3 cell lines treated with samples obtained from PC-3 and A549 cells, respectively. The EV-formulations obtained from PC-3 cells (EVs, EV-PTX, EV-Virus, EV-Virus-PTX) have been used to treat A549 cells, while EV-formulations obtained from A549 cells (EVs, EV-PTX, EV-Virus, EV-Virus-PTX) have been used to treat PC-3 cells in order to carry out the cross-experiments. In both experiments, it was observed that the cell killing effect of the EV formulations is not cancer cell line dependent (Fig 5CD) ($p < 0{,}001$).

3.5. Different molecular mechanisms underlying the anti-neoplastic effects produced by EV-Virus and EV-Virus-PTX treatments

For the evaluation of the molecular mechanisms underlying the enhanced antitumor effect observed between viral and paclitaxel treatments delivered with EVs, we carried out an RNA-SEQ

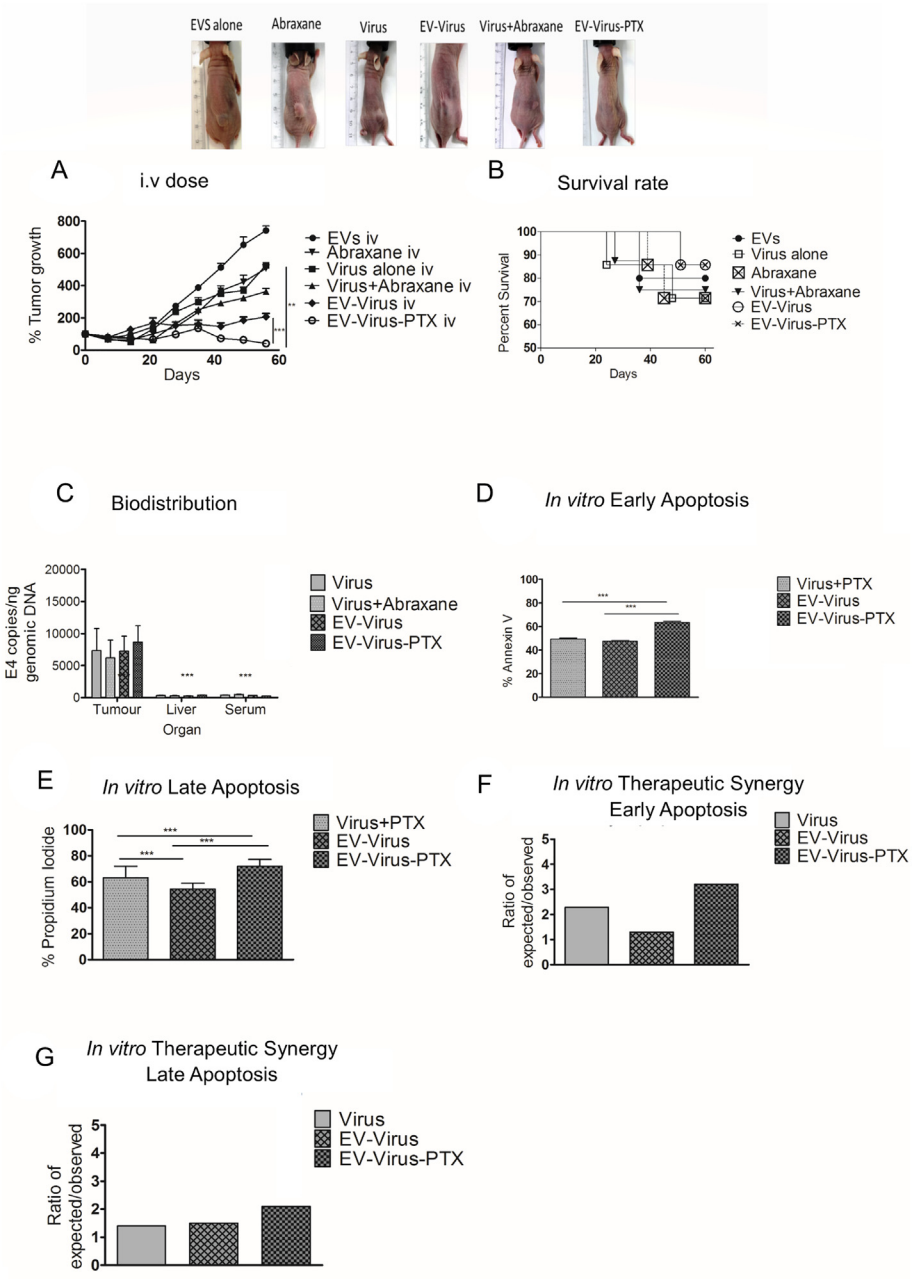

Fig. 2. *In vitro* and *in vivo* enhanced antitumor effects of oncolytic virus and paclitaxel encapsulated in Extracellular vesicles for lung cancer treatment.(A) A549 cell line was implanted subcutaneously into the right flank of BALB/c nude mice. All treatments were administered intravenously (i.v.). Tumor growth was followed over time. (B) Kaplan-Meier test was used to calculate the survival profile. (C) Adenoviral copies towards E4 gene were measured by qPCR from euthanized mice's organs (tumor, liver and serum) at the end of the treatment. (D-E) Early and late apoptotic or necrotic cell death were measured in A549 cells after 24 h post-treatment. The amount of early and late apoptotic or necrotic cells were analyzed by flow cytometry 24 h after the treatments. FITC-labeled Annexin-V was used to indicate the early apoptotic cell and PI for the necrotic or late apoptotic cells, $***P < 0.001$. (F-G) The assessment of the *in vitro* therapeutic synergy was calculated with FTV method. Observed FTV (mean value of experimental cell viability)/(mean value of cell viability control). Expected FTV (mean FTV of Experimental condition)/(mean FTV of experimental control). A ratio > 1 indicates a synergistieffect, and a ratio < 1 indicates a less than additive effect).

transcriptomic analysis on the RNAs extracted from tumor xenografts grown in EV, EV-Virus and EV-Virus-PTX treated mice. The analysis was carried out for 3 samples/group with the only exception of the EV-Virus group for which only 2 samples were of sufficient quality to be analyzed due to the small ratio of human *versus* mouse mRNA extracted from the xenograft. The analysis identified 615 and 317 transcripts for EV-Virus-PTX and EV-Virus treatments, respectively, as differentially expressed in the two conditions, when compared to the EV control treatment. Most of the differentially expressed genes were up-regulated in the EV-Virus, while the majority were down-regulated in the EV-Virus-PTX groups (Fig. 6A). Among the differentially expressed genes only 47 were differentially modulated by both treatments (Fig. 6B) as also detailed in the heat-maps (Fig. 6C). The two distinct genetic programs triggered by EV-Virus and EV-Virus-PTX indicated that a differential cellular response was produced by the two treatments. Indeed, although the types of biological processes involved in the response appeared remarkably similar for both treatments (Supplementary Table 3), the genes dysregulated were different. A general consideration on the net effect produced by the differential expression in terms of up- and down-regulation of each pathway is somehow hampered by the complexity of signals like “metabolic process” or “cellular component organization”. However, were the analysis was possible like for example for the mitogenic pathway, it was clear that both treatments triggered an anticancer effect while regulating different set of genes (Supplementary Fig. 3). In the mitogenic pathway, for example among the genes modulated by EV-Virus-PTX treatment, USP37, SNX33 and POLE were down regulated, whereas overexpression of these genes was shown to induce proliferation by promoting G1/S phase transition [50]; S-phase progression and mitosis respectively [51]. A net anti-proliferative effect was suggested also considering the genes differentially expressed by the EV-Virus treatment, which involves down regulation of BRSK2 expression, known to increase the percentage of cells in G2/M when overexpressed [52], and the upregulation of E2F4, a factor negatively influencing the G1 progression through cell cycle [53]. In conclusion,

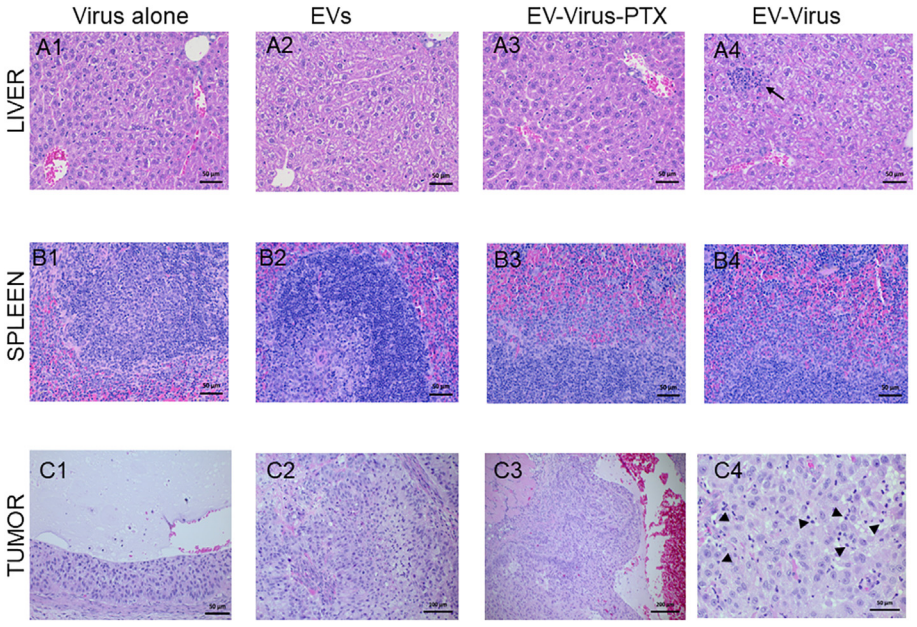

Fig. 3. Histopathological examination on liver, spleen and tumor. (A-C) Liver samples from mice treated with Virus (A1), EVs (A2), EV-Virus-PTX (A3) or EV-Virus (A4) exhibited no significant histopathological findings.A liver sample from an EV-Virus -treated mouse (A4) shows a background lesion; a moderate-sized inflammatory focus (mostly neutrophils; arrow) in otherwise normal liver lobule. (B1) Spleen samples from mice treated with virus alone exhibit mild lymphocytehyperplasia (lymphatic follicles with lymphoblast-like cells, mitotic figs and tingible body macrophages), while spleen samples (B2) from mice treated with extracellular vesicles alone show no significant findings. Typical for nude mice, the PALS area (lightly-staining zone in white pulpa surrounding blood vessels) is sparse and marginal zone inconspicuous. In addition, no secondary follicles are present. (B3) A representative spleen sample from a mice treated with EV-Virus-PTX displays mild hyperplasia of the marginal zone without lymphatic hyperplasia and a sample (B4) from mouse treated with EV-Virus mild hyperplasia of the marginal zone with mild lymphocyte hyperplasia. (C1) Tumor samples from mice treated with virus alone show necrotic remnants of cells in a small necrotic area and apoptotic cell remnants in degenerative area. (C2) A large cavity is filled with proteinacous fluid and lined by cubic to flattened cell. No necrosis. Tumor capsule (C3) A tumor sample treated with EV-Virus-PTX exhibits a large cavity with intraluminal blood and proteinacous fluid.Tumor tissue grows in densely packed nests or packets, and peripheral cords. No necrosis is present. (C4) Tumor sample treated with EV-Virus displays large number of neutrophils (arrowheads; examples) among foamy neoplastic cells.

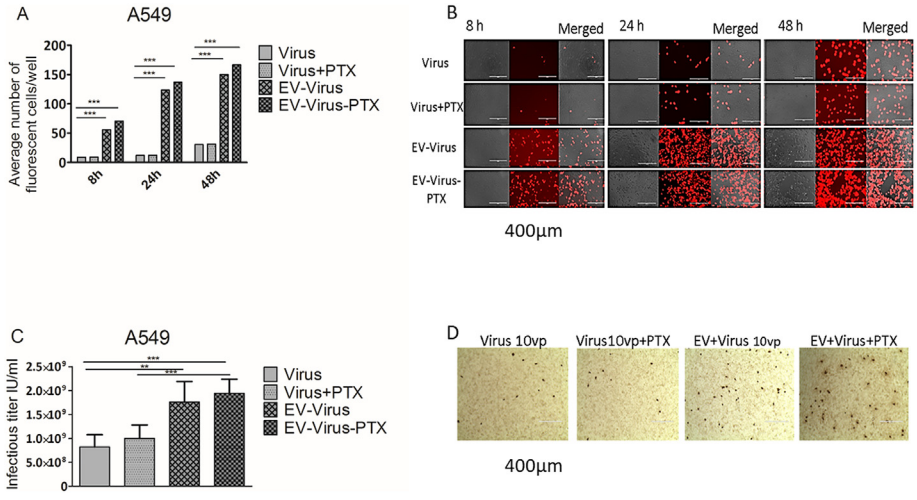

Fig. 4. Effect of oncolytic adenovirus encapsulated into extracellular vesicles on cell transduction and infectivity. (A) The transduction efficacy was evaluated by infection with an oncolyitc adenovirus encoding for the red fluorescent protein (RFP) encapsulated into the extracellular vesicles loaded or not with PTX.RFP was measured using Varioskan plate reader after 8, 24 and 48 h post infection, *** $P < 0.001$. (B) Most representative fluorescent microscope photograph (400 µm) of the infected cells. (C) The infectivity of virus alone, Virus + PTX, EV-Virus and EV-Virus-PTX were assessed by ICC assay. (D) Most representative microscope photographs (400 µm) of the infected wells are presented. Figs represent difference in hexon protein expression (virus assembling), without distinguishing infectivity, replication, or gene expression manner, *** $P < 0.001$. (For interpretation of the references to colour in this fig legend, the reader is referred to the web version of this article.)

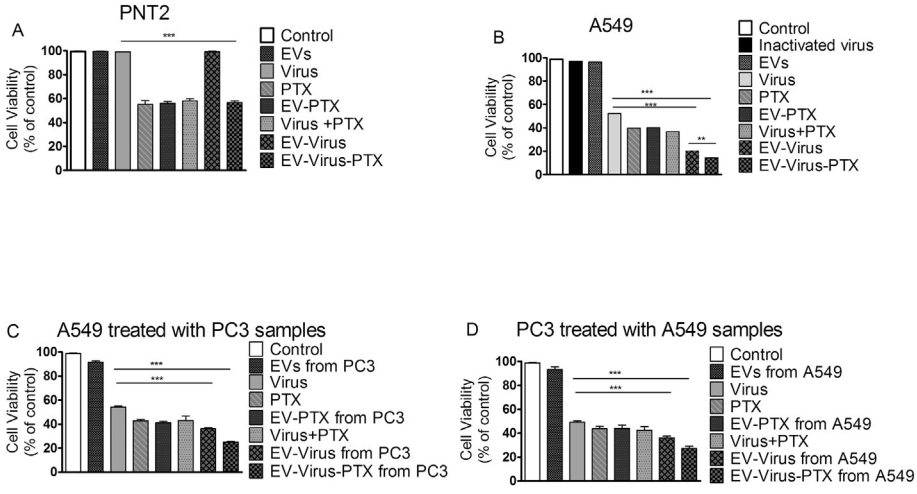

Fig. 5. Effect of oncolytic adenoviruses encapsulated into extracellular vesicles on cell viability. (A-B) Cell viability was performed by MTS assay on PNT2 and A549 cell lines. The absorbance was measured with a 96-wells plate spectrophotometer Varioskan Flash Multimode Reader at 490 nm. (C-D) Cell viability was performed by MTS assay on A549 and PC-3, respectively treated with samples from PC-3 cells and A549 cell lines. EV-formulations from PC-3 cell line tested in A549 cell line: control EVs, EV-PTX, EV-Virus, EV-Virus-PTX. Other formulations tested in A549 cell line: Virus alone, PTX, Virus + PTX. EV-formulations from A549 cell line tested in PC-3 cell line: control EVs, EV-PTX, EV-Virus, EV-Virus-PTX. Other forumulations tested in PC-3 cell line: Virus alone, PTX, Virus + PTX.

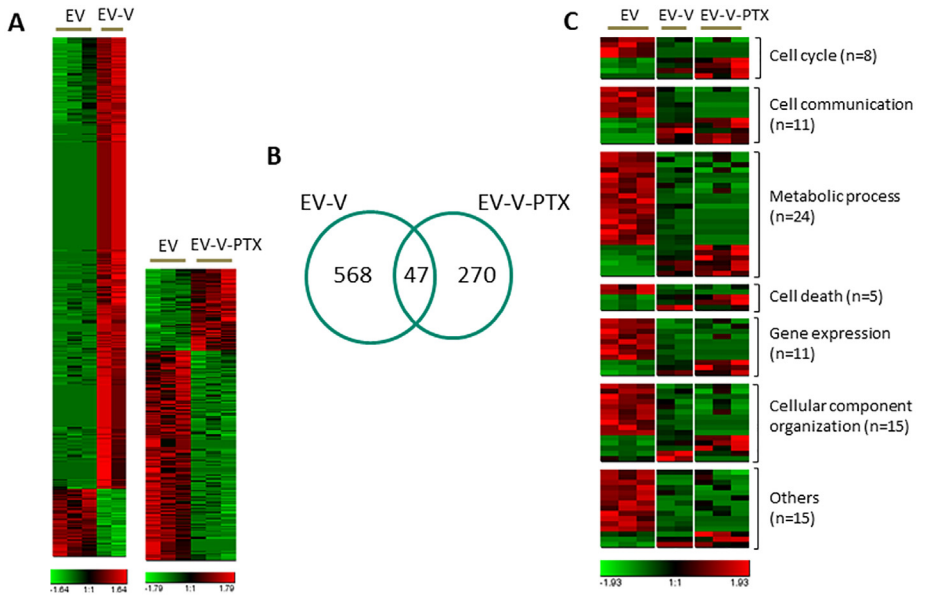

Fig. 6. Transcriptomic analysis.(A) The gene expression profile is represented as heat map (red, high relative expression; black, mean expression; green, low relative expression) showing the expression of up- and down-regulated genes for EV-Virus (615 transcripts) and EV-Virus-PTX (317 transcripts) treatment group, each compared to EV treatment. (B) Venn diagram showing the number of unique and common (47) genes differentially expressed in the EV-Virus andEV-Virus-PTX treatment groups. (C) Heat map showing the expression of 47 common genes subdivided according to the GO terms (Cellular Processes). Sample/group: EV $n = 3$, EV-Virus $n = 2$, EV-Virus-PTX $n = 3$. Cell cycle, cell communication, metabolic process, cell death, gene expression and cellular component organization are the categories with high level of overlapping (number of common genes > 5). (For interpretation of the references to colour in this fig legend, the reader is referred to the web version of this article.)

our transcriptomic analysis suggested that the addition of PTX in the therapeutic EV-Virus-PTX complex is inducing a novel anti-tumor mechanism, which is likely the basis of the observed enhanced*in vivo* antitumor effects and*in vitro* synergistic effect.

4. Discussion

Despite the improvements made in the last years in early detection methods and treatment modalities, lung cancer is still often diagnosed at an advanced stage with poor prognosis and inefficient treatment options [54]. Oncolytic viruses form a potentially powerful anticancer tool, especially when used in combination with other antitumor agents, for advanced cancer patients [14, 15].The systemic delivery of oncolytic viruses is a key factor in order to allow the agent to reach disseminated tumor deposits [55]. However, many early clinical trials have failed since low attention was focused to the features of the delivery process [56]. One possibility is to combine oncolytic viruses with nanoparticle delivery approaches since in systemic delivery, targeting with nanoparticles may focus the viral load to both primary and metastatic tumors to ensure an efficient initial infection [57].Even if current studies have emphasized intratumoral delivery, the systemic delivery seems to be required for the treatment of metastatic cancer [58]. The intratumoral injection of viruses and therapeutic agents has also disadvantages due to the low efficacy and the inability to treat solid and metastatic tumors where the systemic delivery is required [6] [59].

Our system represents a strategy for the systemic delivery of both oncolytic virus and paclitaxel by the cancer cells originated EVs. Herein, the use of cancer-derived EVs represented a proof-of-concept model, since functional studies showed that cancer cells originated EVs have specific cell tropism to their own tumors [60]. However other major challenges for the EVs therapeutic applicability remain, such as the short circulation time of intravenously injected EVs and the possible unspecific accumulation in liver and lung. Given that, to possibily increase the circulation time and have possible involvement in tumor accumulation, it was proposed a post-insertion of EVs with nanobody PEG-micelles as a promising tool for the EVs accumulation in targeted tissues and to improve their potential use in drug delivery [61]. Although EVs have multiple advantages when exploited as a drug delivery vehicles [62, 63], due to their role as regulators in intercellular communication [64, 65], there is still limited knowledge related to scalable isolation, purification methods, as well as criteria for quality analyses of EV-based therapeutics [24, 27, 66, 67]. According to the minimal information for studies of EVs (MISEV), the selection of a method for isolation and purification should be focused on the scientific question and down-stream steps [68]. However, we have set up a system where EVs are produced by large-scale two compartments bioreactor to reduce the workload of EVs production.

Indeed it has been shown that cells use EVs to remove harmful DNA, including DNA originating from adenoviral infection, as a mechanism to protecet themselves [69]. This and our observations raise the question, whether there exist EVs from infected cells that carry only viral DNA without the viral capsid, therefore acting as an alternative delivery vector for the viral DNA for infection, where also the size of the EVs *versus* Virus becomes irrelevant. However as it has not been clarified until this moment, we cannot further comment on this alternative in the light of our current study, however this aspect should be investigated further.

Recently, an increased transduction efficiency for adenoviral vectors encapsulated in anionic liposomes *via* calcium-induced phase-change was reported [70]. Based on this incentive, we checked whether oncolytic viruses expressing red fluorescent protein encapsulated into the EVs (either with or without loaded PTX) have an effect on the transduction efficacy. Notably, already at 8 h post-infection the EV-Virus and EV-Virus-PTX complex groups showed enhanced transduction efficacy in comparison to naked virus as measured by the number of fluorescent cells over other groups.EV-Virus and EV-Virus-PTX complexes also appear to have greater infectivity than virus alone, according to the assay for the infectious titer, which, to some extent, is dependent on the higher efficiency of virus entry into the lung cancer cell line [71] and, since the transduction was enhanced, it has an impact on the improved infectivity.

These results suggest that EVs can greatly improve the delivery of oncolytic viruses to tumor cells.Further, EV-infected cells, as well as cells infected by the conventional route, will produce not only viruses but also EV-Virus complexes that can subsequently infect other tumor cells in its vicinity. Accordingly, the surfaces of EV-Virus infected cells were covered with vesicle-like protrusions while a similar phenotype was absent in uninfected cells. This phenotype may partly derive from virus-induced vesicle formation during apoptosis. Indeed it is still not clear at which apoptotic stage these protrusions have been observed since this phenotype did not always appear, however when it did, it was there at least after 24 h post-infection. In the future, it would be important to characterize the proteome from those vesicles that enclose virus particles in order to determine whether they have unique constituents or if their contents match to those of apoptotic bodies or other types of EVs. Also, given the efficacy of EV-mediated transduction, it

could be possible that (non-enveloped) viruses, or probably just their naked genomes, may spread *via* EVs within the host organism. Combined treatment of oncolytic adenovirus and paclitaxel have been shown to have significantly higher efficacy both *in vitro* and *in vivo* in comparison to oncolytic virus therapy alone [17, 72, 73]. The role of paclitaxel in EV-Virus-PTX complex was to enhance anticancer effect when combined with oncolytic adenoviruses and finally encapsulated into the EVs. We hypothesized that combined agents into the same formulations could exhibit even stronger anticancer effect, as it is known that oncolytic adenoviruses are novel antitumor agents with the ability to selectively replicate in and lyse cancer cells while being harmless for the rest of the body [74] and paclitaxel, an antitumor drug that plays a key role in cancer chemotherapy [75].

It has been already reported that the intratumoral injection of paclitaxel reduces tumor growth in A549 tumor xenograft mice [76]. Additionally, it has been demonstrated that PTX-loaded EVs are more effective in inhibiting the growth of Lewis lung carcinoma metastases than Taxol, a commercial formulation of PTX [77]. Given especially the here-demonstrated increased antitumor efficacy *in vivo*, the combination of paclitaxel and adenovirus in our EV-formulation based delivery approach should similarly exhibit stronger *in vitro* anticancer effect. In order to evaluate possible improved antitumor effect, in local and systemic delivery, we studied the anti-tumor activity of Virus alone, and Virus-PTX encapsulated into EVs, in a lung cancer xenograft model using both intratumoral (i.t.) and intravenous injection (i.v.). I.t. administration of EV-Virus-PTX resulted in tumor growth reduction. Interestingly systemic (i.v.) administration exhibited even stronger antineoplastic activity in lung cancer xenograft mouse model. This is in line with previous experiments showing that intravenous treatment of EV loaded with chemotherapeutic agents can be effective [78]. Importantly, at the end point which was not due to death, metastasis were not macroscopically observed in xenograft murine organs [79]. Furthermore any abnormal clinical signs were observed during the study. Indeed, we found that EV-Virus-PTX was able to induce apoptosis and necrosis showing synergistic antitumor effect *in vitro*.

In turn, based on the *in vitro* cancer cell cross-experiment studies with the PC-3 and A549 we have observed that the cancer cell origins of EVs does not have impact on cancer cell EV delivery properties and killing efficacy in at least the two cancer types used. Our cancer cell cross-experiment results are preliminary; however, they showed, that independently of the origin of the cancer cell line EVs used, they are effective in both cases. This suggests, that the EVs as drug carriers could have versatile applications. Furthermore, the EV-Virus-PTX formulation was able to locally replicate inside tumor, suggesting that viruses administered within EVs could indeed act as self-renewing drug *in situ*, making them especially lucrative candidates for treating metastatic cancer since any metastatis were detected in our *in vivo* animal experiments. However, even if an absolute comparisonbetween virus treatments and EV treatments is not possible with the strategy we used, we find that it can be used to make a conservative comparison for the amounts of viral and EV particles since we did not have more EVs compared to the virus control, and since EV-Virus and EV-Virus-PTX treatments were more effective, this result cannot therefore be explained by a higher dose compared to the virus control.

The molecular mechanism underlying the ability of PTX to enhance the anticancer effect produced by the virus administered in combination with EVs is far from being identified: however, our RNA-SEQ analysis provides some insights showing for the first time that a differential anti-neoplastic mechanism is operating when virus is alone in comparison to being together with PTX in the therapeutic complex. Indeed, PTX was not just contributing with additional gene regulation, but was completely changing the intracellular nodes of the cancer-related pathways targeted by the treatment. Transcriptomic differences observed between EV-Virus and EV-Virus-PTX groups may reflect differences in treatment schedule, however we believe it is very unlikely that an additional fourth treatment with EV-Virus alone at day 15 would produce the enhanced effect on tumor growth observed in the EV-Virus-PTX group; an additional treatment with EV-Virus was expected to produce an additive effect, thus, we consider a better explanation for the enhanced effect the presence of PTX in the formulation,. Future studies are needed to investigate the reasons why PTX in the complex is able to change these intracellular targets thus creating the condition for the enhanced antitumor effect.

5. Conclusions

As a proof of concept, we have demonstrated that cancer cell-derived EVs could be useful vehicles for systemic drug delivery of oncolytic viruses and paclitaxel in the treatment of lung cancer.

We showed that an autologous EV-mediated delivery provides a selective cancer cell tropism andcontributes to enhancing PTX anticancer effects *in vitro* and *in vivo*. Finally, our transcriptomic data suggested that a novel cellular response is triggered by the encapsulation of PTX in the EV-Virus formulation. This response blocked more sensitive nodes in cancer relevant pathways and may thus explain enhanced antitumor effect. All together our study strongly supports the systemic administration of EV-Virus-PTX formulation as new therapeutic strategy aimed at treating lung cancer.

Supplementary data to this article can be found online at https://doi.org/10.1016/j.jconrel.2018.05.015.

Aknowledgments

We thank FCLAP pathologists Hanna-Kaisa Sihvo DECVMP, DVM and Jere Lindén DVM, for histopathological evaluation of the samples. Made Consulting wants to respect the animal technician Anitta Niittymäen's memory and owns the *in vivo* part her memories.

Financial support by grants from Post doc pool foundation (016947-3) and Tekes 3D-Nano-MiniT-project (M.G.), Tekes EV-Extra-Tox and 3D-Nano-MiniT projects (P·S), Academy of Finland and Emil Aaltonen Foundation (M.J. and K.K.), Italian Association for Cancer Research grant IG-11903 (P·C), Orion Foundation, Professor pool (M.Y.), Alfred Kordelin and Eemil Aaltonen Foundations (H.S.).

References

[1] S.M. Gadgeel, S.S. Ramalingam, G.P. Kalemkerian, Treatment of lung Cancer, Radiol. Clin. N. Am. 50 (2012) 961–974, http://dx.doi.org/10.1016/j.rcl.2012.06.003.

[2] H. Lemjabbar-Alaoui, O.U. Hassan, Y.-W. Yang, P. Buchanan, Lung cancer: biology and treatment options, Biochim. Biophys. Acta Rev. Cancer 1856 (2015) 189–210, http://dx.doi.org/10.1016/j.bbcan.2015.08.002.

[3] J.C.C. Hu, R.S. Coffin, C.J. Davis, N.J. Graham, N. Groves, P.J. Guest, K.J. Harrington, N.D. James, C.A. Love, I. McNeish, L.C. Medley, A. Michael, C.M. Nutting, H.S. Pandha, C.A. Shorrock, J. Simpson, J. Steiner, N.M. Steven, D. Wright, R.C. Coombes, A phase I study of OncoVEXGM-CSF, a second-generation oncolytic herpes simplex virus expressing granulocyte macrophage colony-stimulating factor, Clin. Cancer Res. 12 (2006) 6737–6747, http://dx.doi.org/10.1158/1078-0432.CCR-06-0759.

[4] H. Fukuhara, Y. Ino, T. Todo, Oncolytic virus therapy: a new era of cancer treatment at dawn, Cancer Sci. 107 (2016) 1373–1379, http://dx.doi.org/10.1111/cas.13027.

[5] D.Y. Sze, T.R. Reid, S.C. Rose, Oncolytic virotherapy, J. Vasc. Interv. Radiol. 24 (2013) 1115–1122, http://dx.doi.org/10.1016/j.jvir.2013.05.040.

[6] P.K. W. and B.J.C. Russell, Stephen J, Oncolytic Virotherapy, (Jul 10;30 (n.d.)).

[7] T. Ranki, T. Joensuu, E. Jäger, J. Karbach, C. Wahle, K. Kairemo, T. Alanko, K. Partanen, R. Turkki, N. Linder, J. Lundin, A. Ristimäki, M. Kankainen, A. Hemminki, C. Backman, K. Dienel, M. von Euler, E. Haavisto, T. Hakonen, J. Juhila, M. Jaderberg, P. Priha, L. Vassilev, A. Vuolanto, S. Pesonen, Local treatment of a pleural mesothelioma tumor with ONCOS-102 induces a systemic antitumor CD8 $^{+}$ T-cell response, prominent infiltration of CD8 $^{+}$ lymphocytes and Th1 type polarization, Oncoimmunology. 3 (2014) e958937, , http://dx.doi.org/10.4161/21624011.2014.958937.

[8] T. Ranki, S. Pesonen, A. Hemminki, K. Partanen, K. Kairemo, T. Alanko, J. Lundin, N. Linder, R. Turkki, A. Ristimäki, E. Jäger, J. Karbach, C. Wahle, M. Kankainen, C. Backman, M. von Euler, E. Haavisto, T. Hakonen, R. Heiskanen, M. Jaderberg, J. Juhila, P. Priha, L. Suoranta, L. Vassilev, A. Vuolanto, T. Joensuu, Phase I study with ONCOS-102 for the treatment of solid tumors - an evaluation of clinical response and exploratory analyses of immune markers, J. Immunother. Cancer 4 (2016) 17, , http://dx.doi.org/10.1186/s40425-016-0121-5.

[9] L. Vassilev, T. Ranki, T. Joensuu, E. Jäger, J. Karbach, C. Wahle, K. Partanen, K. Kairemo, T. Alanko, R. Turkki, N. Linder, J. Lundin, A. Ristimäki, M. Kankainen, A. Hemminki, C. Backman, K. Dienel, M. von Euler, E. Haavisto, T. Hakonen, J. Juhila, M. Jäderberg, P. Priha, A. Vuolanto, S. Pesonen, Repeated intratumoral administration of ONCOS-102 leads to systemic antitumor CD8+ T-cell response and robust cellular and transcriptional immune activation at tumor site in a patient with ovarian cancer, Oncoimmunology. 4 (2015) 1–5.

[10] C. Larson, B. Oronsky, J. Scicinski, G.R. Fanger, M. Stirn, A. Oronsky, T.R. Reid, Going viral: a review of replication-selective oncolytic adenoviruses, Oncotarget 6 (2015) 19976–19989, http://dx.doi.org/10.18632/oncotarget.5116.

[11] F. McCormick, Cancer-specific viruses and the development of ONYX-015, Cancer Biol. Ther. 2 (2003) 157–160 (doi:216 [pii).

[12] T. Zhao, X. Rao, X. Xie, H.S. Zhou, Adenovirus with insertion-mutated E1A selectively propagates in liver Cancer cells and destroys tumors in vivo advances in brief adenovirus with insertion-mutated E1A selectively propagates in liver Cancer cells and destroys tumors in vivo 1, Cancer Res. (2003) 3073–3078.

[13] P. Forget, J. Vandenhende, M. Berliere, J.P. MacHiels, B. Nussbaum, C. Legrand, M. De Kock, Do intraoperative analgesics influence breast cancer recurrence after mastectomy? A retrospective analysis, Anesth. Analg. 110 (2010) 1630–1635, http://dx.doi.org/10.1213/ANE.0b013e3181d2ad07.

[14] K. Ottolino-Perry, J.-S. Diallo, B.D. Lichty, J.C. Bell, J. Andrea McCart, Intelligent design: combination therapy with oncolytic viruses, Mol. Ther. 18 (2010) 251–263, http://dx.doi.org/10.1038/mt.2009.283.

[15] V. Cerullo, M. Vähä-Koskela, A. Hemminki, Oncolytic adenoviruses, Oncoimmunology. 1 (2012) 979–981, http://dx.doi.org/10.4161/onci.20172.

[16] M.A. Liebert, S. Virus, T. Icp, M. Hsv, T. Toyoizumi, R. Mick, A.E. Abbas, E.H. Kang, L.R. Kaiser, K.L. Molnar-kimber, Combined Therapy with Chemotherapeutic Agents and Herpes Simplex Virus Type 1 ICP34.5 Mutant (HSV-1716) in Human Non-Small Cell Lung Cancer, vol. 3029, (1999), pp. 3013–3029.

[17] S.C. Cheong, Y. Wang, J.-H. Meng, R. Hill, K. Sweeney, D. Kirn, N.R. Lemoine, G. Halldén, E1A-expressing adenoviral E3B mutants act synergistically with chemotherapeutics in immunocompetent tumor models, Cancer Gene Ther. 15 (2008) 40–50, http://dx.doi.org/10.1038/sj.cgt.7701099.

[18] D.P. Eisenberg, NIH Public Access, 8 (2007), pp. 603–615.

[19] M. Yamamoto, D.T. Curiel, Current issues and future directions of oncolytic adenoviruses, Mol. Ther. 18 (2010) 243–250, http://dx.doi.org/10.1038/mt.2009.266.

[20] R. Vile, D. Ando, D. Kirn, The oncolytic virotherapy treatment platform for cancer: unique biological and biosafety points to consider, Cancer Gene Ther. 9 (2002) 1062–1067, http://dx.doi.org/10.1038/sj.cgt.7700548.

[21] L. Kuryk, E. Haavisto, M. Garofalo, C. Capasso, M. Hirvinen, S. Pesonen, T. Ranki, L. Vassilev, V. Cerullo, Synergistic anti-tumor efficacy of immunogenic adenovirus ONCOS-102 (Ad5/3-D24-GM-CSF) and standard of care chemotherapy in preclinical mesothelioma model, Int. J. Cancer 139 (2016) 1883–1893, http://dx.doi.org/10.1002/ijc.30228.

[22] L. Kuryk, L. Vassilev, T. Ranki, A. Hemminki, A. Karioja-Kallio, O. Levälampi, A. Vuolanto, V. Cerullo, S. Pesonen, Toxicological and bio-distribution profile of a GM-CSF-expressing, double-targeted, chimeric oncolytic adenovirus ONCOS-102 – support for clinical studies on advanced cancer treatment, PLoS ONE 12 (2017) 1–15.

[23] H. Saari, E. Lázaro-Ibáñez, T. Viitala, E. Vuorimaa-Laukkanen, P. Siljander, M. Yliperttula, Microvesicle- and exosome-mediated drug delivery enhances the cytotoxicity of paclitaxel in autologous prostate cancer cells, J. Control. Release 220 (2015) 727–737, http://dx.doi.org/10.1016/j.jconrel.2015.09.031.

[24] P. Vader, E.A. Mol, G. Pasterkamp, R.M. Schiffelers, Extracellular vesicles for drug delivery, Adv. Drug Deliv. Rev. 106 (2016) 148–156, http://dx.doi.org/10.1016/j.addr.2016.02.006.

[25] M. Yáñez-Mó, P.R.-M. Siljander, Z. Andreu, A.B. Zavec, F.E. Borràs, E.I. Buzas, K. Buzas, E. Casal, F. Cappello, J. Carvalho, E. Colás, A. Cordeiro-Da Silva, S. Fais, J.M. Falcon-Perez, I.M. Ghobrial, B. Giebel, M. Gimona, M. Graner, I. Gursel, M. Gursel, N.H.H. Heegaard, A. Hendrix, P. Kierulf, K. Kokubun, M. Kosanovic, V. Kralj-Iglic, E.-M. Krämer-Albers, S. Laitinen, C. Lässer, T. Lener, E. Ligeti, A. Line, G. Lipps, A. Llorente, J. Lötvall, M. Manček-Keber, A. Marcilla, M. Mittelbrunn, I. Nazarenko, E.N.M. Nolte't, T.A. Hoen, L.O. Nyman, M. Driscoll, C. Olivan, E. Oliveira, H.A. Pállinger, J. Del Portillo, M. Reventós, E. Rigau, M. Rohde, F. Sammar, N. Sánchez-Madrid, K. Santarém, M.S. Schallmoser, W. Ostenfeld, R. Stoorvogel, S.G. Stukelj, M. Van Der Grein, M.H.M. Helena Vasconcelos, O. De Wever Wauben, Biological properties of extracellular vesicles and their physiological functions, J. Extracell. Vesicles 4 (2015) 1–60.

[26] P. Vader, X.O. Breakefield, M.J.A. Wood, Extracellular vesicles: emerging targets for cancer therapy, Trends Mol. Med. 20 (2014) 385–393, http://dx.doi.org/10.1016/j.molmed.2014.03.002.

[27] S.I. Ohno, G.P.C. Drummen, M. Kuroda, Focus on extracellular vesicles: development of extracellular vesicle-based therapeutic systems, Int. J. Mol. Sci. 17 (2016), http://dx.doi.org/10.3390/ijms17020172.

[28] L. Ran, X. Tan, Y. Li, H. Zhang, R. Ma, T. Ji, W. Dong, T. Tong, Y. Liu, D. Chen, X. Yin, X. Liang, K. Tang, J. Ma, Y. Zhang, X. Cao, Z. Hu, X. Qin, B. Huang, Delivery of oncolytic adenovirus into the nucleus of tumorigenic cells by tumor microparticles for virotherapy, Biomaterials 89 (2016) 56–66, http://dx.doi.org/10.1016/j.biomaterials.2016.02.025.

[29] V. Cerullo, I. Diaconu, V. Romano, M. Hirvinen, M. Ugolini, S. Escutenaire, S.-L. Holm, A. Kipar, A. Kanerva, A. Hemminki, An oncolytic adenovirus enhanced for toll-like receptor 9 stimulation increases antitumor immune responses and tumor clearance, Mol. Ther. 20 (2012) 2076–2086, http://dx.doi.org/10.1038/mt.2012.137.

[30] L. Farzad, V. Cerullo, S. Yagyu, T. Bertin, A. Hemminki, C. Rooney, B. Lee, M. Suzuki, Combinatorial treatment with oncolytic adenovirus and helper-dependent adenovirus augments adenoviral cancer gene therapy, Mol. Ther. Oncolytics 1 (2014) 1–9, http://dx.doi.org/10.1038/mto.2014.8\rhttp://www.nature.com/articles/mto20148#supplementary-information.

[31] R. Jannat, D. Hsu, G. Maheshwari, Inactivation of Adenovirus Type 5 by Caustics, (2005), pp. 446–450.

[32] C. Capasso, M. Hirvinen, M. Garofalo, D. Romaniuk, L. Kuryk, T. Sarvela, A. Vitale, M. Antopolsky, A. Magarkar, T. Viitala, T. Suutari, A. Bunker, M. Yliperttula, A. Urtti, V. Cerullo, Oncolytic adenoviruses coated with MHC-I tumor epitopes increase the antitumor immunity and efficacy against melanoma, Oncoimmunology. 5 (2016) 1–11, http://dx.doi.org/10.1080/2162402X.2015.1105429.

[33] M. Garofalo, B. Iovine, L. Kuryk, C. Capasso, M. Hirvinen, A. Vitale, M. Yliperttula, M.A. Bevilacqua, V. Cerullo, Oncolytic adenovirus loaded with L-carnosine as novel strategy to enhance the antitumor activity, Mol. Cancer Ther. 15 (2016) 651–660, http://dx.doi.org/10.1158/1535-7163.MCT-15-0559.

[34] R.A. Übersichtsarbeit, C. Jackisch, H. Lück, J. Bischoff, Breast Care Weekly Nab -Paclitaxel in Metastatic Breast Cancer – Summary and Results of an Expert Panel Discussion, (2012), pp. 137–143, http://dx.doi.org/10.1159/000338273.

[35] A. Koski, L. Kangasniemi, S. Escutenaire, S. Pesonen, V. Cerullo, I. Diaconu, P. Nokisalmi, M. Raki, M. Rajecki, K. Guse, T. Ranki, M. Oksanen, S.-L. Holm, E. Haavisto, A. Karioja-Kallio, L. Laasonen, K. Partanen, M. Ugolini, A. Helminen, E. Karli, P. Hannuksela, S. Pesonen, T. Joensuu, A. Kanerva, A. Hemminki, Treatment of cancer patients with a serotype 5/3 chimeric oncolytic adenovirus expressing GMCSF, Mol. Ther. 18 (2010) 1874–1884, http://dx.doi.org/10.1038/mt.2010.161.

[36] K.-Y. Tso, S. Lee, K.-W. Lo, K.Y. Yip, Are special read alignment strategies necessary and cost-effective when handling sequencing reads from patient-derived tumor xenografts? BMC Genomics 15 (2014) 1172, http://dx.doi.org/10.1186/1471-2164-15-1172.

[37] A. Dobin, C.A. Davis, F. Schlesinger, J. Drenkow, C. Zaleski, S. Jha, P. Batut, M. Chaisson, T.R. Gingeras, STAR: Ultrafast universal RNA-seq aligner, Bioinformatics 29 (2013) 15–21, http://dx.doi.org/10.1093/bioinformatics/bts635.

[38] S. Anders, P.T. Pyl, W. Huber, HTSeq-A Python framework to work with high-throughput sequencing data, Bioinformatics 31 (2015) 166–169, http://dx.doi.org/10.1093/bioinformatics/btu638.

[39] M.E. Ritchie, B. Phipson, D. Wu, Y. Hu, C.W. Law, W. Shi, G.K. Smyth, Limma powers differential expression analyses for RNA-sequencing and microarray studies, 43 (2018), http://dx.doi.org/10.1093/nar/gkv007.

[40] C. Trapnell, A. Roberts, L. Goff, G. Pertea, D. Kim, D.R. Kelley, H. Pimentel, S.L. Salzberg, J.L. Rinn, L. Pachter, Differential gene and transcript expression analysis of RNA-seq experiments with TopHat and cufflinks, Nat. Protoc. 7 (2013) 562–578, http://dx.doi.org/10.1038/nprot.2012.016.Differential.

[41] J. Jung, T. Mori, C. Kobayashi, Y. Matsunaga, T. Yoda, M. Feig, Y. Sugita, GENESIS: a hybrid-parallel and multi-scale molecular dynamics simulator with enhanced sampling algorithms for biomolecular and cellular simulations, Wiley Interdiscip. Rev 5 (2015) 310–323, http://dx.doi.org/10.1002/wcms.1220.

[42] A. Sturn, J. Quackenbush, Z. Trajanoski, Genesis: cluster analysis of microarray data, Bioinformatics 18 (2002) 207–208, http://dx.doi.org/10.1093/bioinformatics/18.1.207.

[43] H. Xu, X. Niu, Q. Zhang, L. Hao, Y. Ding, W. Liu, L. Yao, Synergistic antitumor efficacy by combining adriamycin with recombinant human endostatin in an osteosarcoma model, Oncol. Lett. 2 (2011) 773–778, http://dx.doi.org/10.3892/ol.2011.334.

[44] Y. Yokoyama, M. Dhanabal, A.W. Griffioen, V.P. Sukhatme, S. Ramakrishnan, Synergy between angiostatin and endostatin: inhibition of ovarian cancer growth, Cancer Res. 60 (2000) 2190–2196.

[45] Y. Benjamini, Y. Hochberg, Controlling the false discovery rate: a practical and powerful approach to multiple testing, J. R. Stat. Soc. B. 57 (1995) 289–300.

[46] W. Gradishar, Albumin-bound paclitaxel: a next-generation taxane, Expert. Opin. Pharmacother. 7 (8) (2006) 1041–1053.

[47] N.A. Rizvi, G.J. Riely, C.G. Azzoli, V.A. Miller, K.K. Ng, J. Fiore, G. Chia, M. Brower, R. Heelan, M.J. Hawkins, M.G. Kris, Phase I/II Trial of Weekly Intravenous 130-Nm Albumin- Bound Paclitaxel as Initial Chemotherapy in Patients with Stage IV Non – Small-Cell Lung Cancer, vol. 26, (2018), pp. 639–643, http://dx.doi.org/10.1200/JCO.2007.10.8605.

[48] H. Chen, X. Huang, S. Wang, X. Zheng, J. Lin, P. Li, L. Lin, Nab-Paclitaxel (Abraxane) -Based Chemotherapy to Treat Elderly Patients with Advanced Non-small-Cell Lung Cancer : ASingle Center, Randomized and Open-Label Clinical Trial, vol. 27, (2015), pp. 190–196, http://dx.doi.org/10.3978/j.issn.1000-9604.2014.12.17.

[49] S.A. Elmore, Enhanced histopathology of the immune system, Toxicol. Pathol. 40 (2012) 148–156, http://dx.doi.org/10.1177/0192623311427571.

[50] X. Huang, M.K. Summers, V. Pham, J.R. Lill, J. Liu, G. Lee, D.S. Kirkpatrick, P.K. Jackson, G. Fang, V.M. Dixit, Deubiquitinase USP37 is activated by CDK2 to antagonize APCCDH1 and promote S phase entry, Mol. Cell 42 (2011) 511–523, http://dx.doi.org/10.1016/j.molcel.2011.03.027.

[51] Z.F. Pursell, T.A. Kunkel, Chapter 4 DNA Polymerase ε. A Polymerase of Unusual Size (and Complexity), (2008).

[52] R. Li, B. Wan, J. Zhou, Y. Wang, T. Luo, X. Gu, F. Chen, L. Yu, APC/C Cdh1 Targets Brain-Specific Kinase 2 (BRSK2) for Degradation via the Ubiquitin-Proteasome Pathway, 7 (2012).

[53] C. Bertoli, J.M. Skotheim, R.A.M. De Bruin, G. Street, HHS Public Access, 14 (2015), pp. 518–528, http://dx.doi.org/10.1038/nrm3629.Control.

[54] A.J. Alberg, J.M. Samet, Epidemiology of lung Cancer * epidemiology of lung Cancer *, Chest 123 (2003) 21S–49S, http://dx.doi.org/10.1378/chest.123.1.

[55] L.W. Seymour, K.D. Fisher, Oncolytic Viruses : Finally Delivering, 114 (2016), pp. 357–361, http://dx.doi.org/10.1038/bjc.2015.481.
[56] K. Fisher, Striking out at disseminated metastases: the systemic delivery of oncolytic viruses, Curr. Opin. Mol. Ther. 8 (2006) 301–313 http://europepmc.org/abstract/MED/16955693.
[57] N. Mendez, V. Herrera, L. Zhang, F. Hedjran, R. Feuer, S.L. Blair, W.C. Trogler, T.R. Reid, A.C. Kummel, Encapsulation of adenovirus serotype 5 in anionic lecithin liposomes using a bead-based immunoprecipitation technique enhances transfection efficiency, Biomaterials 35 (2014) 9554–9561, http://dx.doi.org/10.1016/j.biomaterials.2014.08.010.
[58] F.R. Khuri, J. Nemunaitis, I. Ganly, J. Arseneau, I.F. Tannock, L. Romel, M. Gore, J. Ironside, R.H. MacDougall, C. Heise, B. Randlev, A.M. Gillenwater, P. Bruso, S.B. Kaye, W.K. Hong, D.H. Kirn, A controlled trial of intratumoral ONYX-015, a selectively-replicating adenovirus, in combination with cisplatin and 5-fluorouracil in patients with recurrent head and neck cancer, Nat. Med. 6 (2000) 879–885.
[59] L. Aurelian, Oncolytic virotherapy: the questions and the promise, Oncolytic Virotherapy. 2 (2013) 19–29, http://dx.doi.org/10.2147/OV.S39609.
[60] A. Hoshino, B. Costa-silva, T. Shen, G. Rodrigues, A. Hashimoto, M.T. Mark, H. Molina, S. Kohsaka, A. Di Giannatale, S. Ceder, S. Singh, C. Williams, N. Soplop, K. Uryu, L. Pharmer, T. King, L. Bojmar, A.E. Davies, Y. Ararso, T. Zhang, H. Zhang, J. Hernandez, J.M. Weiss, V.D. Dumont-cole, K. Kramer, L.H. Wexler, Tumour exosome integrins determine organotropic metastasis, Nature 527 (2015) 329–335, http://dx.doi.org/10.1038/nature15756.
[61] S.A.A. Kooijmans, L.A.L. Fliervoet, R. Van Der Meel, M.H.A.M. Fens, H.F.G. Heijnen, P.M.P. Van Bergen, P. Vader, R.M. Schiffelers, PEGylated and Targeted Extracellular Vesicles Display Enhanced Cell Specificity and Circulation Time, 224 (2016), pp. 77–85, http://dx.doi.org/10.1016/j.jconrel.2016.01.009.
[62] K. Tang, Y. Zhang, H. Zhang, P. Xu, J. Liu, J. Ma, M. Lv, D. Li, F. Katirai, G.-X. Shen, G. Zhang, Z.-H. Feng, D. Ye, B. Huang, Delivery of chemotherapeutic drugs in tumour cell-derived microparticles, Nat. Commun. 3 (2012) 1282, , http://dx.doi.org/10.1038/ncomms2282.
[63] J.P.K. Armstrong, M.N. Holme, M.M. Stevens, Re-Engineering Extracellular Vesicles as Smart Nanoscale Therapeutics, (2017), http://dx.doi.org/10.1021/acsnano.6b07607.
[64] G. Camussi, M.C. Deregibus, S. Bruno, V. Cantaluppi, L. Biancone, Exosomes/microvesicles as a mechanism of cell-to-cell communication, Kidney Int. 78 (2010) 838–848, http://dx.doi.org/10.1038/ki.2010.278.
[65] S.W. Ferguson, J. Nguyen, Exosomes as therapeutics : the implications of molecular composition and exosomal heterogeneity, J. Control. Release 228 (2016) 179–190, http://dx.doi.org/10.1016/j.jconrel.2016.02.037.
[66] G. Fuhrmann, A. Lena, I.K. Herrmann, European journal of pharmaceutics and biopharmaceutics extracellular vesicles – a promising avenue for the detection and treatment of infectious diseases ? Eur. J. Pharm. Biopharm. 118 (2017) 56–61.
[67] T. Lener, M. Gimona, L. Aigner, V. Börger, E. Buzas, G. Camussi, N. Chaput, D. Chatterjee, F.A. Court, H.A. Portillo, L.O. Driscoll, S. Fais, J.M. Falcon, U. Felderhoff-mueser, L. Fraile, Y.S. Gho, R.C. Gupta, A. Hendrix, D.M. Hermann, A.F. Hill, F. Hochberg, P.A. Horn, D. De Kleijn, L. Kordelas, B.W. Kramer, S. Lanerplamberger, S. Laitinen, T. Leonardi, M.J. Lorenowicz, S.K. Lim, J. Lötvall, C.A. Maguire, A. Marcilla, I. Nazarenko, T. Patel, S. Pedersen, G. Pocsfalvi, S. Pluchino, P. Quesenberry, I.G. Reischl, F.J. Rivera, R. Sanzenbacher, K. Schallmoser, I. Slaper-cortenbach, D. Strunk, T. Tonn, Applying Extracellular Vesicles Based Therapeutics in Clinical Trials – An ISEV Position Paper, (2015), p. 3078, http://dx.doi.org/10.3402/jev.v4.30087.
[68] K.W. Witwer, C. Soekmadji, A.F. Hill, M.H. Wauben, E.I. Buzás, D. Di Vizio, J.M. Falcon-perez, C. Gardiner, F. Hochberg, I.V. Kurochkin, J. Lötvall, S. Mathivanan, S. Sahoo, H. Tahara, A.C. Torrecilhas, A.M. Weaver, H. Yin, L. Zheng, Y.S. Gho, P. Quesenberry, E.I. Buzás, D. Di Vizio, J.M. Falcon-perez, C. Gardiner, F. Hochberg, V. Kurochkin, J. Lötvall, S. Mathivanan, R. Nieuwland, S. Sahoo, Updating the MISEV minimal requirements for extracellular vesicle studies : building bridges to reproducibility, J. Extracell. Vesicles 6 (2017), http://dx.doi.org/10.1080/20013078.2017.1396823.
[69] A. Takahashi, R. Okada, K. Nagao, Y. Kawamata, A. Hanyu, S. Yoshimoto, M. Takasugi, S. Watanabe, M.T. Kanemaki, C. Obuse, *E. Hara*, excreting harmful DNA from cells, Nat. Commun. 8 (2017) 1–14, http://dx.doi.org/10.1038/ncomms15287.
[70] Z. Zhong, S. Shi, J. Han, Z. Zhang, X. Sun, Anionic liposomes increase the efficiency of adenovirus-mediated gene transfer to Coxsackie-adenovirus receptor deficient cells, Mol. Pharm. 7 (2010) 105–115, http://dx.doi.org/10.1021/mp900151k.
[71] P. Sharma, A.O. Kolawole, S.M. Wiltshire, K. Frondorf, K.J.D.A. Excoffon, Accessibility of the coxsackievirus and adenovirus receptor and its importance in adenovirus gene transduction efficiency, J. Gen. Virol. 93 (2012) 155–158, http://dx.doi.org/10.1099/vir.0.036269-0.
[72] A.M. Hassan, S. Braam, F. Kruyt, Paclitaxel and vincristine potentiate adenoviral oncolysis that is associated with cell cycle and apoptosis modulation, whereas they differentially affect the viral life cycle in non-small-cell lung cancer cells, Cancer Gene Ther. 13 (2006) 1105–1114, http://dx.doi.org/10.1038/sj.cgt.7700984.
[73] C.K. Ingemarsdotter, S.K. Baird, C.M. Connell, D. Öberg, G. Halldén, I.A. McNeish, Low-dose paclitaxel synergizes with oncolytic adenoviruses via mitotic slippage and apoptosis in ovarian cancer, Oncogene 29 (2010) 6051–6063, http://dx.doi.org/10.1038/onc.2010.335.
[74] A. Rosewell Shaw, M. Suzuki, Recent advances in oncolytic adenovirus therapies for cancer, Curr. Opin. Virol. 21 (2016) 9–15, http://dx.doi.org/10.1016/j.coviro.2016.06.009.
[75] E. Bernabeu, M. Cagel, E. Lagomarsino, M. Moretton, D.A. Chiappetta, Paclitaxel: what has been done and the challenges remain ahead, Int. J. Pharm. 526 (2017) 474–495, http://dx.doi.org/10.1016/j.ijpharm.2017.05.016.
[76] C. Wang, T. Chen, Intratumoral injection of taxol in vivo suppresses A549 tumor showing cytoplasmic vacuolization, J. Cell. Biochem. 113 (2012) 1397–1406, http://dx.doi.org/10.1002/jcb.24012.
[77] M.S. Kim, M.J. Haney, Y. Zhao, V. Mahajan, I. Deygen, N.L. Klyachko, E. Inskoe, A. Piroyan, M. Sokolsky, S.D. Hingtgen, A.V. Kabanov, E.V. Batrakova, HHS public, Access 12 (2017) 655–664.
[78] S. Xu, Y. Tian, Y. Hu, N. Zhang, S. Hu, D. Song, Z. Wu, Y. Wang, Y. Cui, H. Tang, Tumor growth affects the metabonomic phenotypes of multiple mouse non-involved organs in an A549 lung cancer xenograft model, Sci. Rep. 6 (2016) 28057, , http://dx.doi.org/10.1038/srep28057.
[79] X. Cai, J. Luo, X. Yang, H. Deng, J. Zhang, S. Li, H. Wei, C. Yang, L. Xu, R. Jin, Z. Li, In Vivo Selection for Spine-Derived Highly Metastatic Lung Cancer Cells is Associated with Increased Migration, Inflammation and Decreased Adhesion, (2015), p. 6.